Available online at www.sciencedirect.com
SCIENCE DIRECT®
Journal of Chromatography B, 808 (2004) 3–14
JOURNAL OF CHROMATOGRAPHY B
www.elsevier.com/locate/chromb

Monoliths for microfluidic devices in proteomics

Séverine Le Gac [a], Julien Carlier [b], Jean-Christophe Camart [b], Cécile Cren-Olivé [a], Christian Rolando [a,*]

[a] *Laboratoire de Chimie Organique et Macromoléculaire, Université des Sciences et Technologies de Lille (Lille 1), UMR CNRS 8009, Chimie Organique et Macromoléculaire, 59655 Villeneuve d'Ascq Cedex, France*
[b] *Institut d'Electronique, de Microélectronique et de Nanotechnologie, Université des Sciences et Technologies de Lille, UMR CNRS 8520, Villeneuve d'Ascq Cedex, France*

Available online 7 June 2004

Abstract

We report here on the preparation of monolithic capillary columns in view to their integration in a microsystem for on-chip sample preparation before their on-line analysis by electrospray and mass spectrometry (ESI–MS). These monolithic columns are based on polymer materials and consist of reverse phases for peptide separation and/or desalting. They were prepared using lauryl methacrylate (LMA), ethylene dimethacrylate (EDMA) as well as a suitable porogenic mixture composed of cyclohexanol and ethylene glycol. The resulting stationary phases present thus a C12-functionality. The LMA-based columns were first prepared in a capillary format using capillary tubing of 75 μm i.d. and tested in nanoLC–MS experiments for the separation of a commercial Cytochrome *C* digest composed of 12 peptidic fragments whose isoelectric point values and hydrophobic character cover a wide range. The LMA-based columns were capable of separating the peptidic fragments and their performances were seen to be similar as those of standard commercial columns dedicated to proteomic purposes with calculated separation efficiencies up to 145×10^3 plates/m. Monolithic LMA-based phases were then successfully polymerized in microchannels fabricated using the negative photoresist SU-8. After the polymerization, the systems were seen to withstand the pressures applied during the nanoLC–MS separation tests that were carried out in the same conditions as for the monolithic capillary columns. The pressure drop during these tests of the in-microchannel monoliths was as high as 50 bar; however, the separation was not as good as for a capillary format which could be accounted for by the monolith dimensions.

Keywords: Polymer monoliths; Microfluidic devices; Miniaturization; Proteomics

1. Introduction

These last years novel miniaturized analytical tools [1,2] are emerging which are referred to as μTAS (Micro-Total Analysis Systems) or Lab-on-a-chip devices. These miniaturized and integrated devices are of great interest in the fields of analytical biology and chemistry [3,4] as they can be used with little handling. Furthermore, sample loss and contamination are decreased. In addition to this, fast, automated and high-throughput analysis is possible. Last, these small devices are appropriate for the analysis of reduced-sized samples like biological ones.

Here we report the development of a microfluidic device dedicated to the preparation of protein samples prior to their on-line analysis by electrospray and mass spectrometry (ESI–MS). The system includes different modules, including a chromatographic device and an integrated ionization emitter tip with the shape of a nib [5] for the introduction of the sample into the mass spectrometer, as illustrated on Fig. 1.

On-chip separations are mostly performed under an electrical field [6]; electro-based pumping systems are easier to implement on a microchip format since no valve is required. Nonetheless, these latter imply the addition of salts in the solution, which are detrimental for the analysis in ESI–MS [7]. Only a few compositions of the mobile phase are acceptable for both the electrochromatography and the

Abbreviations: AcCN, acetonitrile; AIBN, 2,2′-azobisisobutyronitrile; CyOH, cyclohexanol; Cyt C, Cytochrome *C*; EG, ethylene glycol; EDMA, ethylene dimethacrylate; HCOOH, formic acid; HV, high voltage; IDA, information dependant acquisition; LMA, lauryl methacrylate; MeOH, methanol; SEM, scanning electron microscopy; SPE, solid phase extraction; SU-8, name of a photoresist used for microtechnology processes.

* Corresponding author. Tel.: +33-3-20-43-49-77; fax: +33-3-20-33-61-36; mobile: +33-6-60-67-37-78.
E-mail address: christian.rolando@univ-lille1.fr (C. Rolando).

1570-0232/$ – see front matter © 2004 Elsevier B.V. All rights reserved.
doi:10.1016/j.jchromb.2004.03.067

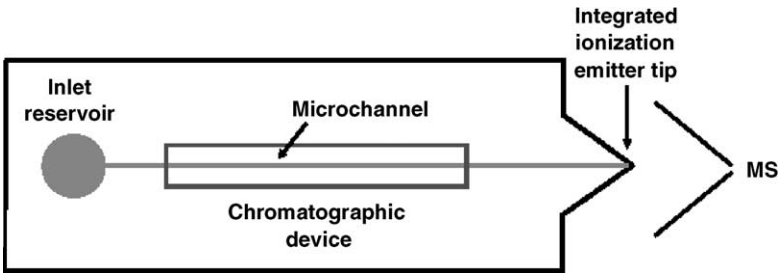

Fig. 1. Schematic representation of the microfluidic system which includes a chromatographic device and an integrated ionization emitter tip with the shape of a nib.

nanoelectrospray ionization, leading to a non-satisfying compromise for real analytical work [8–10]. Here, the flow relies on a hydraulic pumping system, which excludes any electro-driven separation. This implies the use and introduction of a stationary phase in the microchannels, this phase suiting such a microfluidic context. Creating a stationary phase means structuring the microchannel so as to generate a high surface area for the analytes to interact with the solid support. A first idea to achieve that is to pack particles in a section of a microchannel [11]; they are maintained using frits. However, it is difficult to control the packing density of the particles and to introduce frits in a microchannel [12,13]. In addition, frits are prone to clogging and are the site of bubble generation [14]. Bead trapping was also demonstrated using either bars [15] or a kind of restriction in the microchannel [16]. A second idea is to structure the microchannel using microtechnology techniques by etching pillar-shaped structures in it [17]. Nonetheless, this microtechnology-based route does not allow the generation of a surface area which is high enough for chromatographic purposes and, in addition, the fabrication cost is very high for routine production [18]. A third idea that we have chosen for our microfluidic development is to use a monolithic phase, that can be prepared in situ in a microchannel and that is based either on silica or on polymer. Monoliths can be described as interconnected networks of cross-linked and porous globules [19,20] which present a bimodal porosity; large through-pores (>50–100 nm) which consist of the preferential pathway for fluids to flow through the column and small pores (<2 nm) where molecular interactions take place between analytes and stationary place. As the material is monolithic here, there is no restraint in the porosity properties dictated by the packing of spherical particles which usually gives a 26% calculated interstitial void volume in packed columns [19]. These mass transfer limitations linked to diffusion phenomena affect the separation performances in HPLC [21]. In particle-based devices, the liquid flows *around* the particles whereas it flows *through* the material in case of monolithic materials. The resistance to mass transfer is thus lower using this material and can be further promoted by the presence of through-pores greater than 600 nm whereby convection phenomena appear in addition to the usual diffusion ones [22,23]. This results in a faster and enhanced mass transfer. On the contrary, using particle-based columns, mass transfer is only governed by diffusion phenomena. It is hence very slow, especially for high molecular weight analytes and the operating pressure is high as the consequence of the lower porosity.

Polymer macroporous monoliths are prepared using a radical polymerization process initiated either by UV-irradiation or by the temperature. The reaction mixture is composed of (i) monomers, mono-vinylic ones which bear the functionality and poly-vinylic ones which are cross-linking agents, (ii) a porogenic solvent which governs the formation of the porous structure and (iii) an initiator. The monolith structure and porosity are influenced by the porogen content in the reaction mixture, the quantity and quality of the initiator, the ratio mono-/poly-vinylic monomers and the temperature in case of a thermally induced polymerization [24]. Monomers mostly belong to the families of either acrylate [25] compounds or styrene/divinylbenzene [26]. Monolithic phases have found a number of applications mainly as chromatographic stationary phases for any separation mode (normal separation [27], reverse phase separation [28], ion exchange separation [29], affinity separation [30], capillary electrochromatography [31], pressure assisted capillary electrochromatography . . .) and as solid supports for reactors [32]. Compared to their silica-based counterparts [33], polymer-based monoliths withstand a wide range of pH values [34]. In addition, a great variety of chemistry [23] and consequently of separation modes is possible as a result of the large range of functional monomers that can be introduced in the reaction mixture.

So, monoliths present a series of advantages for microfluidic applications [35]; they are prepared in one step in a local way providing the polymerization is initiated by UV-irradiation. Their physical and chemical properties can be adjusted providing some changes in the polymerization mixture composition to fit microfluidic applications. Firstly, their porosity can thus be promoted so as to decrease the pressure drop along the column. Indeed, a too high pressure drop may damage the bonding between the top and the bottom wafers and cannot be provided by an on-chip pumping system. As a consequence, porosity is a critical parameter for materials dedicated to microfluidic applications. Secondly, depending on the application field, the monolith functionality can be tailored. Hence, their use in a microsystem format has already been described as SPE

phases [36], mixing-inducing structures [37], micro-reactor solid supports [38], and reverse phases [39] for electrochromatography (Fig. 1).

We report here on the preparation of monolithic phases for microfluidic applications and especially on the preparation of stationary phases for chromatographic purposes in a reverse-phase separation mode. The monolith polymerization was initiated by UV-irradiation and monoliths were first prepared in a capillary tubing as this consists of a good model for microchannels and then in microchannels that were fabricated in the negative photoresist SU-8. The resulting monolithic columns were first studied for their morphology and porosity properties and then tested for the separation of a Cyt C digest in nanoLC–MS experiments.

2. Experimental

2.1. Materials and chemicals

UVs transparent fused-silica capillary tubing (75 μm i.d.; 360 μm o.d.) was purchased from Polymicro Technologies (Phoenix, AZ). The UV lamp (2 × 20 W, 365 nm, I = 2100 μW/cm^2) was purchased from Elvetec (France). Lauryl methacrylate (LMA), ethylene dimethacrylate (EDMA), 2,2′-azobisisobutyronitrile (AIBN), trimethoxysilylpropylsilane, methanol (MeOH), ethylene glycol (EG), cyclohexanol (CyOH), acetone, sodium hydroxide (NaOH) and hydrochloric acid (HCl) were purchased from Sigma–Aldrich (L'isle d'Abeau, France). The commercial Cytochrome *C* digest was purchased from Dionex (Amsterdam, The Netherlands). Deionized water (18.2 MΩ) was prepared using a Milli-Q system from Millipore (Billerica, MA, USA).

2.2. Monolith preparation in capillary tubing

Capillary tubing was connected to a syringe-pump (Harvard Apparatus, Holliston, MA, USA) using appropriate connections (UpChurch Scientific, Oak Harbour, WA, USA) for the preparation steps. Capillary tubing was treated using a previously described procedure [35]. It was first rinsed with acetone (15 min) and deionized water (15 min), activated by a 0.2 M NaOH solution (30 min), washed again with deionized water (15 min), treated with a 0.2 M HCl solution (30 min) and washed again consecutively with deionized water (15 min) and acetone (15 min) before drying for 90 min (80 °C). Once back to room temperature, the capillary tubing was filled with a 15% vol. 3-trimethoxysilylpropylsilane solution in acetone, closed using appropriate caps (UpChurch Scientific, Oak Harbour, WA, USA) and let for treatment reaction for 24 h at room temperature. After a 2 h acetone washing, the tubing was finally placed overnight in oven (80 °C) for drying. The monomer mixtures and the porogens were first prepared separately and then mixed in the indicated volume ratio; 1% wt. AIBN was then added. The N_2-degased polymerisation mixture was injected in the capillary tubing, which was then closed at its extremities and placed under UV-irradiation for 2 h. Once the reaction was completed, the resulting monolithic phase was abundantly washed with MeOH to remove the un-reacted chemicals and placed overnight in oven (80 °C) for drying.

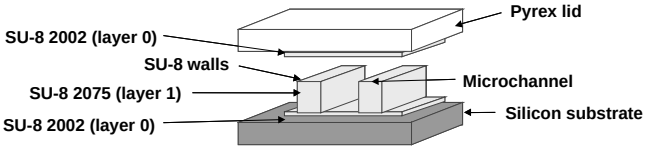

Fig. 2. Schematic representation of the microtechnology route used for the fabrication of the SU-8-based microsystem with a multi-layered structure.

2.3. Microsystem preparation

The microsystems were fabricated using a SU-8-based technology that has been described elsewhere and that mainly relies on a series of standard photolithography steps that allow for forming and patterning the successive layers of SU-8 [40]. The microsystems consist of microchannels made in the negative photoresist SU-8 using photolithography techniques. Fig. 2 illustrates the SU-8 multi-layered structure used to build the microsystem. A first thin layer of SU-8 2002 (2 μm) was deposited on a supporting silicon wafer. On that layer, a second and thick layer of SU-8 2075 (height of ∼200 μm) was deposited as walls having a 200 μm thickness, i.e. to form the microchannel and the accesses for the introduction of the transfer capillary tubing. This layer also includes pillars that support the Pyrex lid and allow for optimizing its bonding on the main SU-8 layer. The microsystem was closed using a Pyrex wafer also coated with a SU-8 2002 layer (2 μm); it was thus bonded on the bottom wafer using a SU-8/SU-8 bonding technique. It should be noted that the two thin layers of SU-8 2002 that were deposited on the supporting Si wafer and the Pyrex lid were introduced in the structure so as to enhance the adhesion of the SU-8 resist walls; this is critical when dealing with high-aspect ratio structures such as microchannels. This wall-based structure allowed to diminish the stresses between the bottom and the top wafer and thus to enhance the wafer bonding together with to prevent from any wafer warping. Fig. 3 is a photograph of one of the resulting microsystems with the wall and pillar structures below the Pyrex lid. The microchannels were of 200 μm depth, of 100–500 μm width and of 3 cm total length. The microsystem was connected to the lab-world using standard fused-silica capillaries coated with polyimide (20 μm i.d.; 150 μm o.d.) so as to facilitate the injection of the chemicals and the coupling for the nanoLC–MS separation tests. These capillaries were introduced in the microchannels at their inlets and outlets and glued in place using a 2-component epoxy glue.

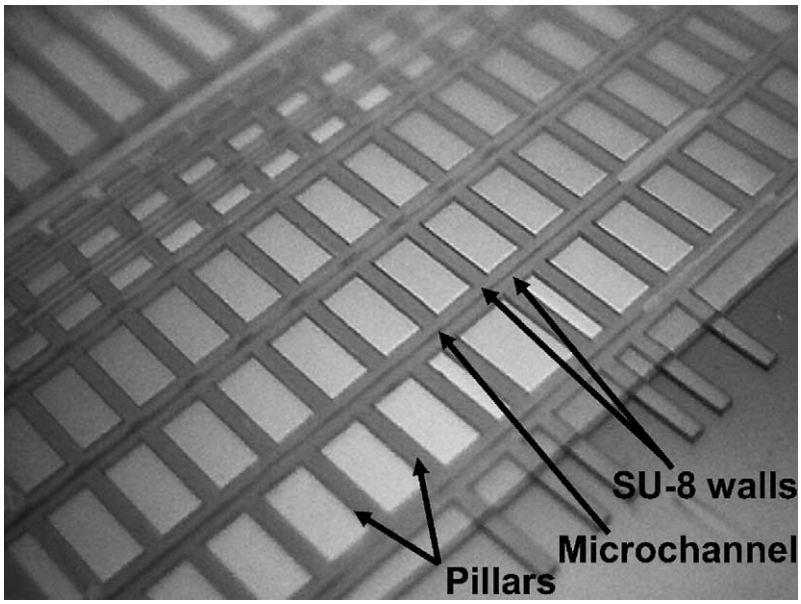

Fig. 3. Photograph of a microsystem made according to the multi-layered structure fabrication route.

2.4. Monolith preparation in microchannels

The monoliths were prepared in microchannels according to the procedure described above for the polymerizations in capillary tubing except from the preliminary inner wall treatment step which was suppressed here. Indeed, the microchannel inner walls did not present any silanol groups as is the case for the fused-silica capillary tubing and there was no chance for the monolith to escape from their support due to the presence of the transfer capillaries at both ends of the microchannels. UV-initiated polymerization was carried out after a mask was placed on both ends of the microchannels. Thus, the 2.8 cm-long microchannel contained a 2.2 cm-long monolithic column.

2.5. Test in nanoLC–MS

The monolithic columns were tested for separation experiments on a nanoLC set-up from LC Packings-Dionex (Amsterdam, The Netherlands) including an Ultimate Micro Pump to pump solvents through the columns, an Accurate stream splitter and a Famos injection system. The separation tests were carried out using a commercial Cytochrome *C* digest (Dionex, Amsterdam, The Netherlands) which was directly injected onto the column without any pre-concentration step. The elution was performed using a gradient of solvent A (95% H_2O, 5% AcCN, 0.1% HCOOH) and solvent B (95% AcCN, 5% H_2O, 0.1% HCOOH), this gradient having been optimized for the separation of the Cytochrome *C* digest on a commercial PepMap column (LC Packings, Amsterdam, The Netherlands): solvent B content was increased from 5 to 50% in 30 min, from 50 to 95% in 1 min, was kept for 5 min at 95% and finally was decreased back to 5% in 1 min. The column was allowed to re-equilibrate for approximately 40 min before another separation test was run. The pressure drop during the nanoLC runs was measured using the Ultimate Micro Pump system and recorded by *Chromeleon* software (LC Packings-Dionex, Amsterdam, The Netherlands). Detection was achieved using mass spectrometry techniques on an API QStar Pulsar Q-q-TOF mass spectrometer (Applied Biosystems, MA, USA). The monolithic column was connected at its outlet to a 50 cm long fused-silica capillary tubing (20 μm i.d.; 280 μm o.d.) using a Teflon butt-to-butt connection (LC Packings-Dionex, Amsterdam, The Netherlands). This transfer capillary tubing was connected at its other end to a fused-silica PicoTip source (20 μm i.d.; 360 μm o.d.; 15 μm i.d. at its tip; New Objective, Cambridge, MA, USA) using the same butt-to-butt Teflon connection as previously. The tip position was adjusted to 1–2 mm in front of the MS inlet. Detection was carried out in positive mode with a 2.2–2.5 kV HV and the spectra were acquired on a *m*/*z* 300–2000 range, the nanoLC set-up being coupled to the mass spectrometer. The data acquisition was controlled by software *Bioanalyst* (Applied Biosystems, MA, USA) in IDA mode with a detection cycle time of 10 s. Fragmentation was triggered for any doubly charged species reaching an intensity threshold of 30 counts with a relative collision energy that had been calculated taking account of the charge state of the selected species and with Ar as collision gas. Once selected and fragmented, eluted species were excluded from the MS/MS selection (± 0.5 Da mass window exclusion around the ion *m*/*z* value) for 1 min.

3. Results and discussion

3.1. Preparation of the monolithic capillary columns

Monolithic columns were first prepared in capillary tubing of 75 μm i.d. which was cut in pieces of 15–20 cm

length. This capillary tubing was seen as a good model of microchannels due to its size close to that of microfabricated channels. It is also an appropriate support for the study of the monolithic phases as it is easily connected to any pumping system using dedicated connectors. We used here capillary tubing which was transparent to UV-irradiation to enable an UV-initiated polymerization for the preparation of the monoliths. Indeed, this polymerisation initiation mode enables a spatial control of the reaction in the microchannels and thus the preparation of columns having a given length using appropriate photomasks. It should be noted that the inner diameter of the capillaries was dictated by the most currently commercially available capillary tubing having an i.d. of 75 μm.

The column preparation and the polymerization process were done in standard conditions as already widely described in the literature with a first preliminary treatment of the inner walls using a heterobifunctional coupling agent which ensures the covalent anchoring of the monolith in its capillary support. Then, the polymerisation mixture was injected into the capillary which was placed under UV-irradiation for around 2 h. The resulting monolithic was abundantly washed using MeOH and dried overnight in an oven. The polymerisation mixture was composed here of LMA and EGDMA (see Fig. 4) as monomers in a 65/35 molar ratio and 60% vol. of porogen composed of cyclohexanol and ethylene glycol in a 80/20 volume ratio. AIBN was last added as 1% wt. of the monomers. The polymerization process was not initiated through a thermal activation. Firstly, wrapping capillary tubing in an aluminium foil prevents the polymerization from proceeding and secondly, when using photomasks for the irradiation of the polymerization mixture, the monolithic column was seen to be polymerized in the irradiated zones and not under the mask, which shows that the polymerization process was induced by UV-irradiation and not in a thermal way (Fig. 4).

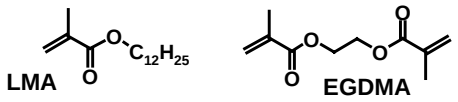

Fig. 4. Monomers used for the polymerization, LMA or lauryl methacrylate as functional monomer and EDMA or ethylene dimethacrylate as cross-linking agent.

3.2. Study of the porosity and morphology properties of the monolith

The monolithic columns prepared in capillary tubing were observed under scanning electron microscopy (SEM). The obtained photograph (Fig. 5) first shows the typical structure of monolithic materials. They are composed of small and interconnected globules which form a monolithic porous structure. The monolithic material presented here has an homogeneous appearance with regularly-shaped and sphere-like small nodules. The size of the globules was roughly determined to be in a 0.6–1.25 μm range, according to an enlarged SEM photograph; it should be noted that this size is more than five-fold less than those of conventional porous particles packed in chromatographic devices,

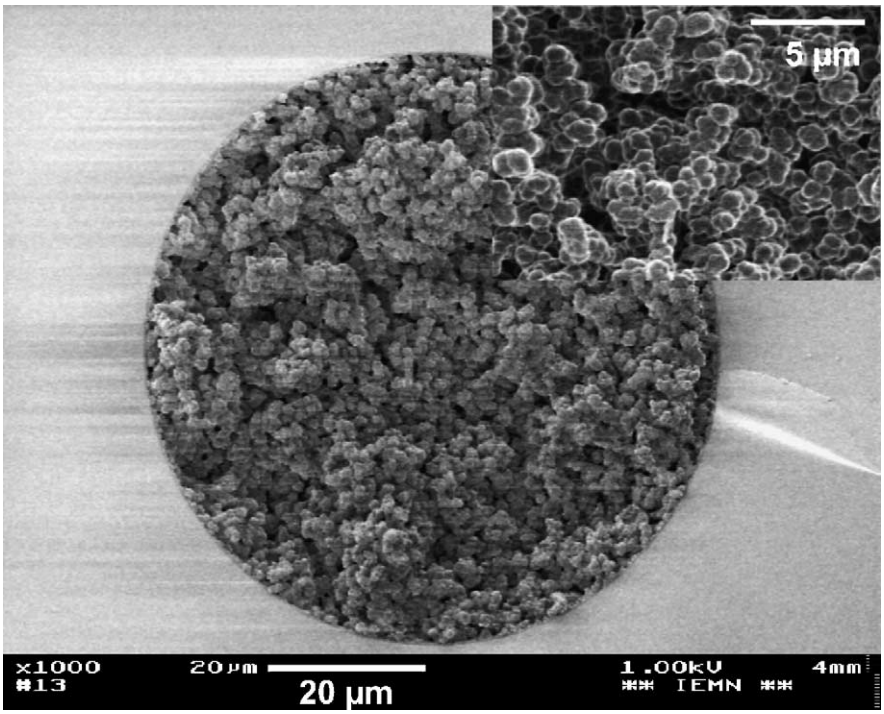

Fig. 5. Scanning electron microscopy (SEM) photograph of a section of capillary tubing which contains a monolithic phase; enlarged view of the monolith morphology in inset.

which authorizes the preparation of narrower columns than when using porous particles. In addition, the column presents a low inter-particular void content and a structure that suits for chromatographic applications as flow-through is not favoured in a too great extent. This monolithic column was prepared using an appropriate porogenic mixture (CyOH/EG 80/20) and presents an appropriate structure for separation purposes with no "large" pores but rather a continuous structure.

The study of the monolith morphology and porosity properties also included the measurement of the pressure drop observed along a column during a separation test (see Fig. 6 for its profile). The typical pattern of the pressure plot $P = f(t)$ presents a plateau with a maximal value, ΔP_{max} when the acetonitrile content is low, i.e. at the beginning and the end of the gradient and a drop when the acetonitrile content was abruptly increased up to 76% (t = 31–36 min, B = 95%). The pattern of this plot is illustrated in Fig. 6 for in-microsystem tests. For the monolithic column tested here the ΔP_{max} value was of 80 bar. This value can be compared to the pressure drop observed when operating a commercial column based on packed silica-particles; this column is of 15 cm and exhibits a pressure drop of 125 bar. As a matter of fact, this P_{max} value is linked to what is called the macroporosity of the column, i.e. the large through-pores of the monolithic phase or the inter-particle voids in a column based on packed particles. It reflects thus the resistance to mass transfer of the column material; this accounts for that P_{max} is higher for a particle-based column as the flow occurs around the particles in the 26% inter-particular void and not through the material. We then calculated the permeability B_0 of our column to compare it to a commercial column based on packed particles, using Darcy's law:

$$B_0 = \frac{\eta L Q}{A\,\Delta P}$$

where L is the column length, Q the fluid flow-rate through the column, A the section area of the column and ΔP the pressure drop along the column expressed in Pascal. B_0 was calculated for the described monolithic column (L = 17 cm, i.d. 75 μm) as well as for a commercial PepMap column (Dionex, *The Netherlands*) (L = 15 cm, i.d. 75 μm). The fluid viscosity was taken as 0.94 mPa s, calculated as the viscosity of a solvent mixture composed of 9.5% AcCN and 90.5% H_2O (95% solvent A and 5% solvent B). These respective values (see Table 1) confirm that monolithic columns are more permeable and that the mass transfer is much higher that with columns based on packed particles In addition, they are in agreement with those indicated in the literature [41]. We then calculated the corresponding mean pore diameter d_p for the column material applying the Kozeny–Carman equation as proposed by Gusev et al. [42]:

$$d_p = 2 \times \sqrt{\frac{5 \times B_0}{\varepsilon_T}}$$

where d_p is the mean pore diameter, B_0 the permeability of the column and ε_T the total porosity of the column. This latter was approximated to be 0.6 for the monolithic column assuming the total porosity was equal to the volume introduced of porogen as a first approximation, and 0.3 for the PepMap column. The coefficient 2 is linked to the shape of the pores which are assumed to be cylindrical and the coefficient 5 is an empirical Kozeny coefficient for such a structure composed of packed sphere particles. The mean pore diameter values calculated using this model gives a 0.7 and 0.5 μm values, respectively, for our monolithic column and a PepMap one. These values agree with the respective pressure drop values measured on both columns: the higher the porosity, the lower the pressure drop. Nonetheless, according to Vervoort et al., the coefficient values must be changed depending on the phase porosity [43] and this formula cannot be used for high-porosity materials ($\varepsilon_T > 0.8$). However, the estimated values for d_p allow us to compare our monolithic column to a PepMap one in terms of mean pore diameter. The calculated value could not be confirmed using the SEM picture of the monolithic phase (Fig. 5); this latter is obtained for a monolith in a dry state whereas the d_p value is calculated for a swollen polymer using the phase permeability and thus a measured pressure drop value and the liquid viscosity (Table 1).

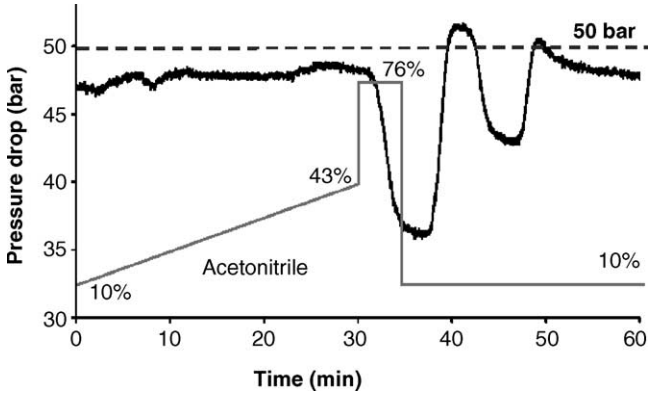

Fig. 6. Pressure drop measured along the in-channels monolithic columns during a separation test using a nanoLC set-up connected to ESI–MS.

3.3. Separation tests using a Cyt C digest sample

Separation tests were carried out against a Cytochrome *C* digest sample which is commercially available. This sample consists of 12 peptidic fragments of bovine Cytochrome *C*, which cover a wide range of physical and chemical properties, such as their molecular weight, iso-electric point (pI) and hydrophobicity (log *P*). Due to these various properties, this digest sample is used to adjust the separation gradient on conventional columns and is a good reference sample to assess the separation capabilities of a chromatographic column. Table 2 summarizes the properties of the 12 fragments contained in the Cytochrome *C* digest.

Table 1
Comparison of the monolithic column discussed here with a commercial PepMap column based on porous silica particles; dimensions of the column (length L and A section area), test parameters (flow-rate Q and maximum of pressure drop ΔP) as well as physical properties (permeability B_0 and mean pore diameter d_p)

	L (cm)	A (μm^2)	Q (nl/min)	ΔP (bar)	B_0 (μm^2)	d_p (μm)
Monolithic column	17	0.44×10^4	200	80	1.51×10^{-2}	0.7
PepMap column	15	0.44×10^4	100	125	0.4×10^{-2}	0.5

Table 2
List of the Cytochrome *C* fragments contained in the commercial digest sample with their sequence, mono-molecular weight, isoelectric point (pI) and hydrophobic character (Kyte–Doolittle scale) calculated using *Expasy* software

Sequence	Fragment sequence	Mass $(M + H)^+$	pI	Hydrophobic character
56–73	GITWGEETLMEYLENPKK	2138.05	4.5	−0.96
56–72	GITWGEETLMEYLENPK	2009.95	4.1	−0.79
9–22	IFVQKCAQCHTVEK	1633.82	8.1	0.02
39–53	KTGQAPGFSYTDANK	1584.77	8.5	−1.19
40–53	TGQAPGFSYTDANK	1456.67	5.5	−0.99
26–38	HKTGPNLHGLFGR	1433.78	11.0	−0.88
89–99	GEREDLIAYLK	1306.7	4.7	−0.61
28–38	TGPNLHGLFGR	1168.62	9.4	−0.39
92–99	EDLIAYLK	964.53	4.1	0.21
80–86	MIFAGIK	779.45	8.5	1.6
74–79	YIPGTK	678.36	8.6	−0.57
9–13	IFVQK	634.39	8.8	0.82

Separation tests were performed on a nanoLC set-up. 1 μl of the Cyt C digest sample (800 or 80 fmol) was directly injected into the column without a first pre-concentration step. Peptides were detected using MS techniques with an on-line coupling of the column to an API QStar Pulsar Q-q-TOF mass spectrometer instead of the UV diode arrays detector. MS is first more sensitive than UV detection and second allows for identifying the eluted species using their molecular weight (deduced from the m/z value read on the mass spectra) or their sequence determined using the MS/MS spectra. Fig. 7 shows the MS trace obtained for the separation of 800 fmol of the Cyt C digest on the LMA-based column that was tested here; the peptidic fragments are well separated as seen on this graph. The reconstructed chromatograms were plotted for all the peptidic fragments, as shown on Fig. 8 as well as the corresponding mass spectra. They were first used to determine the retention time of each peptidic species. We chose not to use the apparent retention

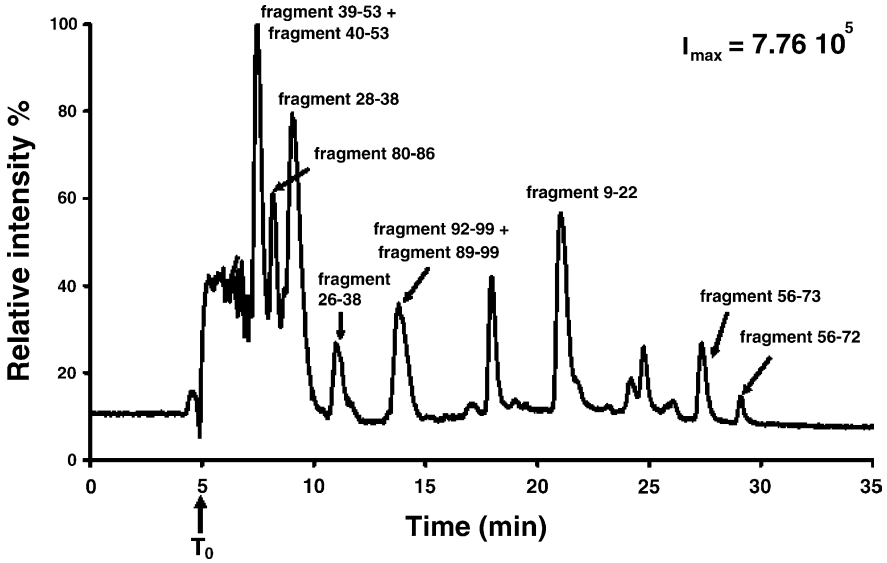

Fig. 7. MS trace of a separation on a LMA-based monolithic column; separation experiment using a Cyt C digest sample at 800 fmol and a 200 nl/min flow-rate. T_0 is indicated as an arrow at the elution start.

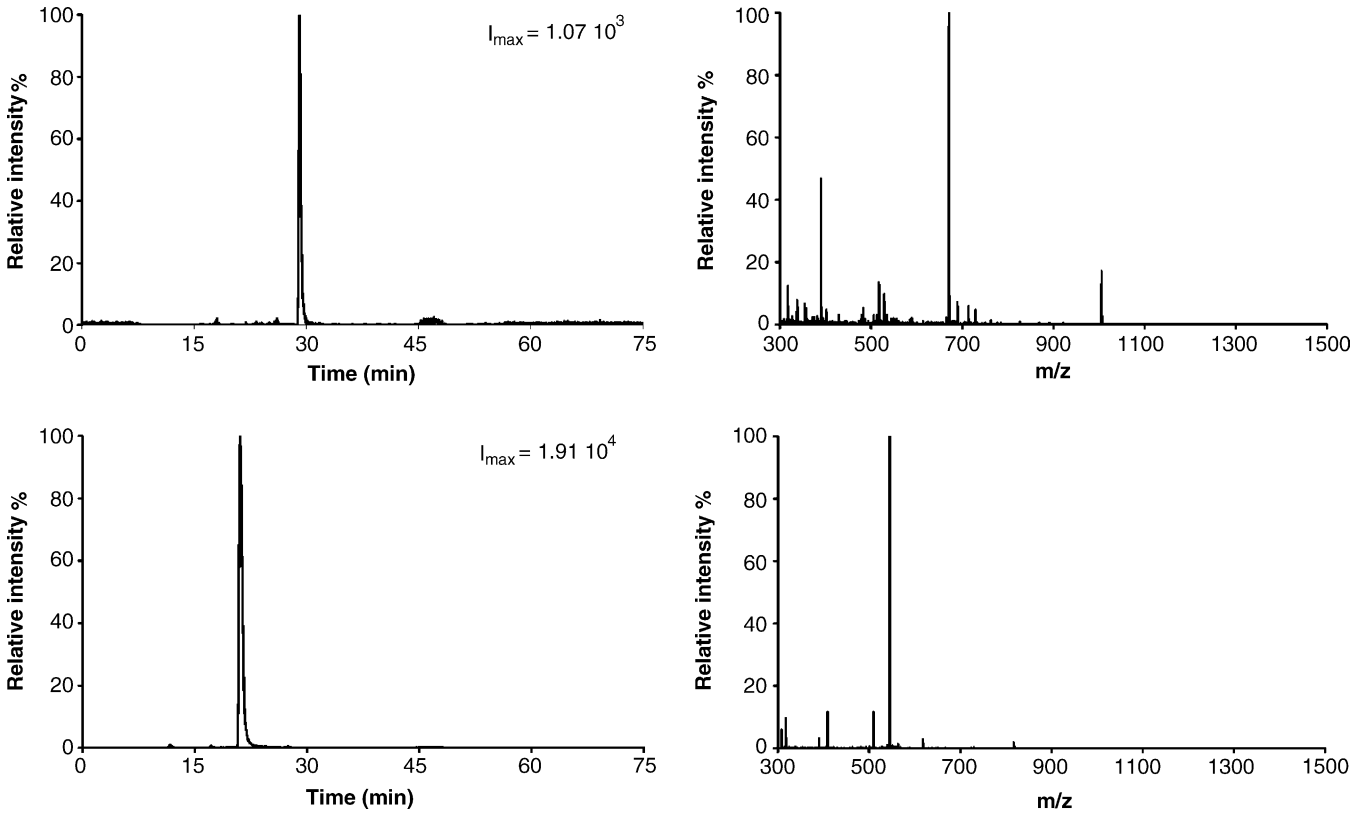

Fig. 8. Reconstructed chromatograms (left) and corresponding mass spectra (right) for two fragments of the Cyt C for the separation based on 800 fmol of digest sample; fragments 56–72 ($T_r - T_0 = 22.06$ min; $N_{rel} = 145 \times 10^3$ plates/m) (top) and 9–22 ($T_r - T_0 = 16.08$ min; $N_{rel} = 66 \times 10^3$ plates/m) (bottom).

time value but a relative retention time T_r defined as $T_r = T_{rapp} - T_0$ where T_0 is the time where elution starts and T_{rapp} the absolute value read on the chromatogram. This allows us to suppress the dead time linked to the coupling of the monolithic capillary column to the mass spectrometer using capillary tubing which increases the retention time values on the MS trace. The reconstructed chromatograms were also used to determine the relative separation efficiency N_{rel}; this latter was calculated using the following formula, assuming a Gaussian peak shape:

$$N_{rel} = 5.54 \times \left(\frac{T_r - T_0}{w}\right)^2$$

where $T_r - T_0$ and w are the relative retention time and calculated peak width at its half-height respectively, and N_{rel} is given as a total number of plates. It should be noted that the relative separation efficiency was calculated here using a relative retention time $T_r - T_0$ which is lower than the absolute retention time T_r. Consequently, the relative efficiency values appear to be lower as they are under-estimated. The inter-test reproducibility was investigated with a series of consecutive separation runs, which allow for assessing the result dispersion. The column performed well and the separation was reproducible from one test to another one. Table 3 summarizes these data for the separated Cytochrome *C* fragments. Separation efficiency should be calculated for an isocratic separation experiment and not a gradient one as we did here as the increased AcCN amount results in narrowing peaks. Nonetheless, the separation results obtained in gradient conditions can be correlated to those obtained in isocratic conditions using the LSS model [44] so as to correct the separation efficiency values. The results presented in Table 3 for the separation of 800 fmol of a Cytochrome *C* sample were seen to correlate well with this model and the curve $N_{rel} = f(T_r - T_0)$ fit an exponential curve with a correlation factor of 0.9224.

The corresponding mass spectra allowed us to determine whether peptides were co-eluted or not and whether peaks overlapped. From these data, it comes out that the LMA-based column discussed here gave a very nice separation of the 12 fragments of the Cyt C digest with separation efficiency values which were comparable to those obtained on a commercial column based on packed silica-particles (PepMap, Dionex, The Netherlands). Nonetheless, it should be noted that the shortest fragments were eluted in the injection peak (fragments 74–79 and 9–13) and are not indicated in Table 3 and that two fragments (fragments 39–53 and 40–53) were co-eluted as shown on the corresponding mass spectra.

Using the same column, a separation test with a 80 fmol Cyt C sample, i.e. 10-fold less material than previously, was carried out. The MS trace was not as nice as this obtained with a more concentrated sample, but the peptidic frag-

Table 3
Separation results on a LMA-based monolithic column for either a 800 fmol sample or a 80 fmol one

Fragment	Test with 800 fmol Cyt C			Test with 80 fmol Cyt C		
	Averaged relative retention time ($T_r - T_0$) (min)[a,d]	Relative efficiency N_{rel} (plate)[b,d]	Relative efficiency N_{rel} (10^3 plate/m)[c,d]	Averaged relative retention time ($T_r - T_0$) (min)[a,d]	Relative efficiency N_{rel} (plate)[b,d]	Relative efficiency N_{rel} (10^3 plate/m)[c,d]
56–72	23.72 ± 0.32	49615 ± 7980	292 ± 47	23.06 ± 0.04	43459 ± 5229	256 ± 31
56–73	22.03 ± 0.26	22599 ± 2761	133 ± 16	21.65 ± 0.05	–[e]	–[e]
9–22	16.04 ± 0.04	9087 ± 2064	53 ± 12	15.91 ± 0.11	16824 ± 3215	99 ± 19
89–99	9.16 ± 0.06	2452 ± 699	14 ± 4	9.17 ± 0.16	4485 ± 44	26.4 ± 0.3
92–99	8.79 ± 0.02	945 ± 33	5.6 ± 0.2	9.11 ± 0.10	–[e]	–[e]
26–38	6.12 ± 0.12	881 ± 79	5.2 ± 0.5	6.35 ± 0.12	2461 ± 44	14 ± 0.3
28–38	4.18 ± 0.04	809 ± 332	4.8 ± 1.9	4.56 ± 0.05	1530 ± 189	9 ± 1.1
80–86	3.27 ± 0.09	1513 ± 854	8.9 ± 5	3.44 ± 0.07	504 ± 3	3.0 ± 0.02
40–53	2.64 ± 0.09	532 ± 75	3.1 ± 0.4	2.68 ± 0.08	1002 ± 15	5.9 ± 0.09
39–53	2.49 ± 0.08	1038 ± 81	6.1 ± 0.5	2.54 ± 0.09	990 ± 30	5.8 ± 0.2

[a] Relative retention time calculated using the reconstructed chromatograms and taken as ($T_r - T_0$) with T_0 being the elution start time.
[b] Relative separation efficiency in number of plates calculated using the peak width at its half-height w and the relative retention time ($T_r - T_0$); $N_{rel} = 5.54 \times ((T_r - T_0)/w)^2$.
[c] Separation efficiency in number of plates/m calculated using the column length ($L = 17$ cm).
[d] Result dispersion assessed using a series of three consecutive tests carried out in the same conditions.
[e] Not determined.

ments were retained on the column and separated. Thus, our monolithic home-made columns are able to separate small amounts of sample like this 80 fmol Cyt C digest sample. As before, we plotted the reconstructed chromatograms for the 12 peptidic fragments contained in the Cyt C digest. Fig. 9 shows the reconstructed chromatograms for some of the Cyt C fragments. As previously, the precise relative retention time $T_r - T_0$ and the relative separation efficiency

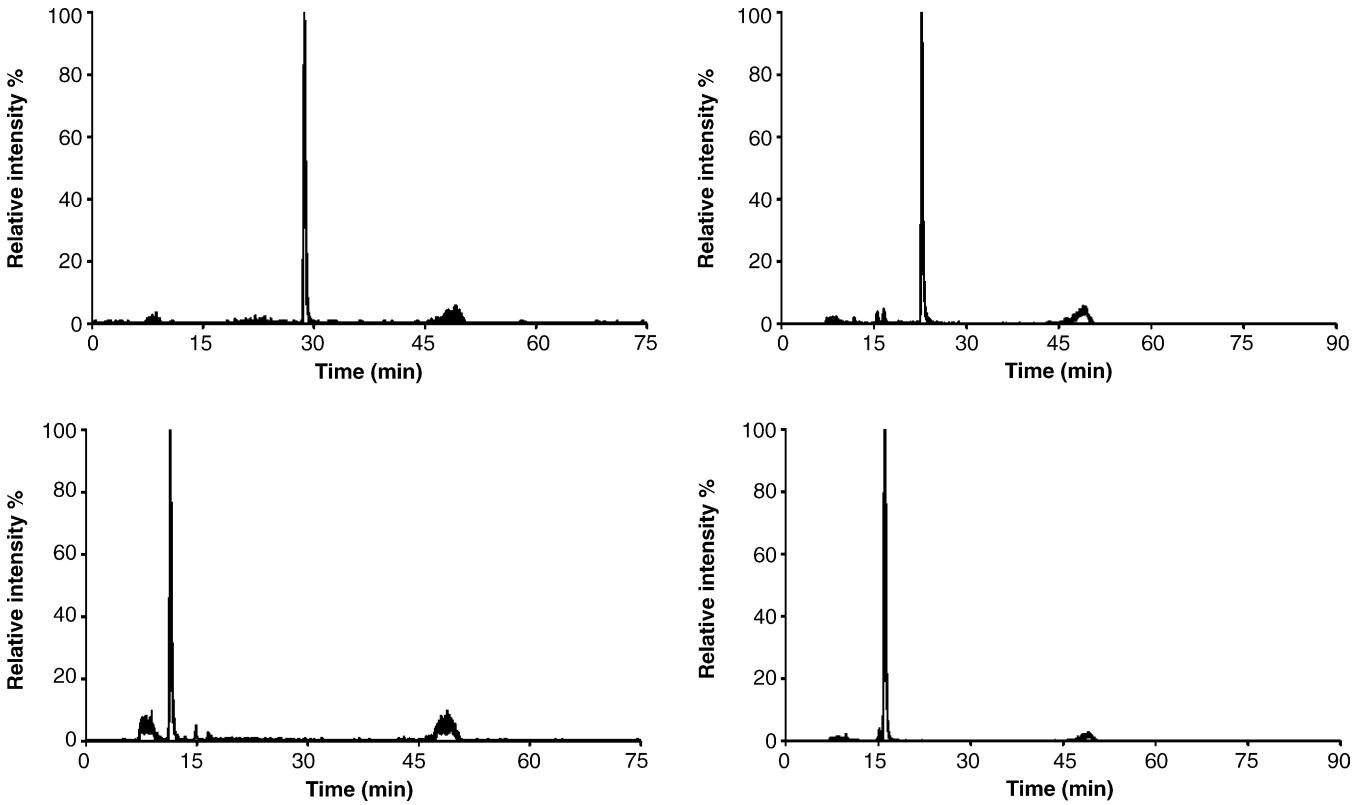

Fig. 9. Examples of reconstructed chromatograms for a series of Cyt C fragments for the separation using 80 fmol of the digest sample (test 1), from left to right and from top to down, fragments 56–73 ($T_r - T_0 = 21.68$ min; $N_{rel} = 325 \times 10^3$ plates/m), fragments 9–22 ($T_r - T_0 = 16.05$ min; $N_{rel} = 97.1 \times 10^3$ plates/m), fragments 28–38 ($T_r - T_0 = 4.58$ min; $N_{rel} = 9.5 \times 10^3$ plates/m), fragments 92–99 ($T_r - T_0 = 9.39$ min; $N_{rel} = 30.4 \times 10^3$ plates/m).

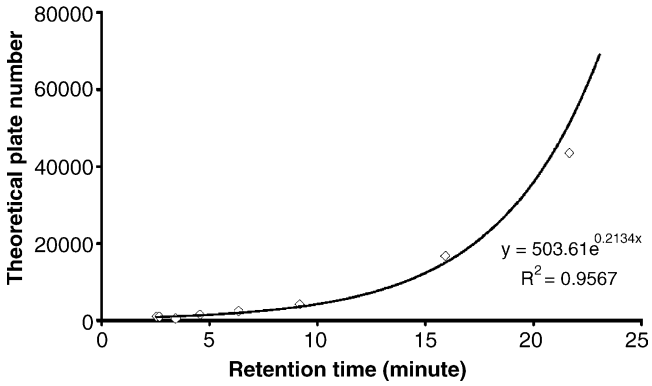

Fig. 10. Correlation between the calculated relative separation efficiency in number of plates and the relative retention time, assuming a logarithmic variation of the retention time for the linear gradient used. Correlation plot obtained for a separation test using 80 fmol of a Cyt C digest sample.

values N_{rel} were calculated for the different separation tests that were carried out and the result dispersion was assessed as well; these values are summarized in Table 3. Again the shortest fragments which are eluted in the injection peak are not mentioned in this Table. It should be observed that the efficiency values are much greater than previously when a 800 fmol sample was run, which demonstrates that the column was saturated for the earlier experiment using a more concentrated sample at 800 fmol/μl. However, the minority peptides are more difficult to detect like fragments 56–72 and 89–99 for example which are hardly detected. As before, we plotted $N_{rel} = f(T_r - T_0)$ which corresponds to an exponential curve. Thus, as for the separation of 800 fmol of Cyt C digest, the separation results fit the model that correlates the efficiency values obtained with a gradient experiment to this of an isocratic separation. Fig. 10 presents the plot $N_{rel} = f(T_r - T_0)$ obtained using the averaged N_{rel} and $(T_r - T_0)$ values which has a correlation factor of 0.9567. The number of plates for an isocratic elution can be assessed to be around a value of 500. This plot also highlights that the gradient composition could be improved with a less steep increase in acetonitrile so as to give a better peptide separation with higher separation efficiency value.

3.4. Separation test in the microsystem

For the tests in microsystems, the same reaction mixture composition was used to prepare the monolithic phase, i.e. a porogen composed of ethylene glycol and cyclohexanol and LMA and EDMA as monomers introduced in a 65/35 molar ratio. Nonetheless, the phase was made more porous by introducing a larger volume of porogen in the reaction mixture, 70% against 60% before. This aimed at preventing from any problems caused by a too high pressure drop along the monolithic column which could result in the rupture of the cover lid bonding. The rupture may be detected as iridescence that appears between the SU-8 walls underneath the Pyrex cover lid caused by the leaking of the liquid outside the microchannels. The in-microsystem polymerisation succeeded as demonstrated by the resulting white trace in the selected channel (see Fig. 11). It should be noted here that no weakness neither of the microsystem nor of the cover lid bonding was observed after some hours pumping and the use of several chemical solutions. This is, to our knowledge, state-of-the-art performances for microfabricated systems, as the system including a polymerized monolith was able to withstand an up to 50 bar pressure drop (Fig. 6) for a whole night nanoLC runs.

The in-microchannel monolithic column was tested in the same conditions as before in nano-LC–MS coupling using

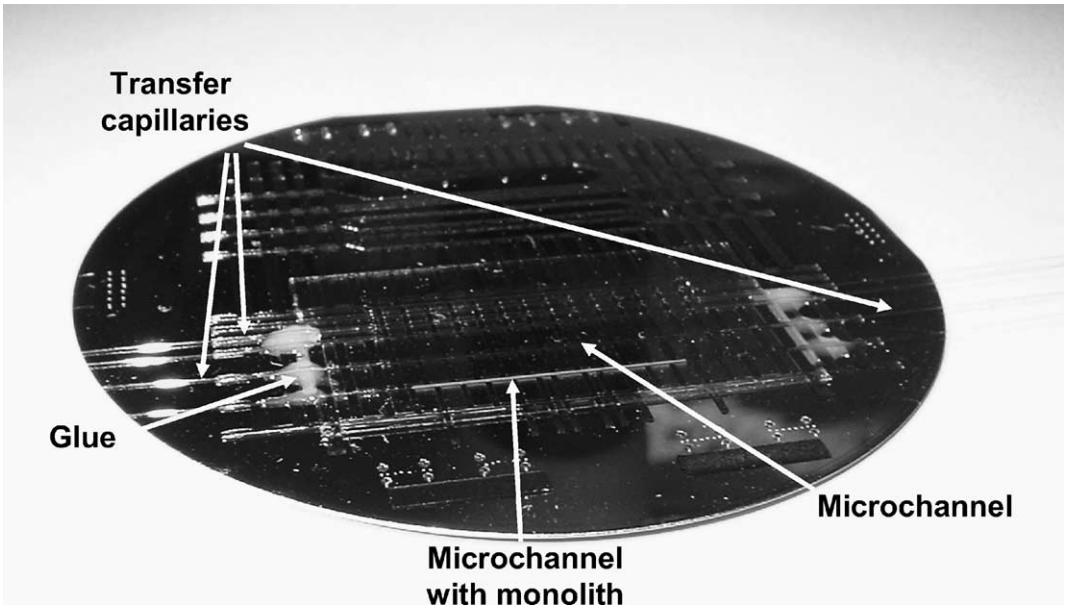

Fig. 11. Photograph of a SU-8-based microsystem including a monolithic column seen as a white trace in the first microchannel.

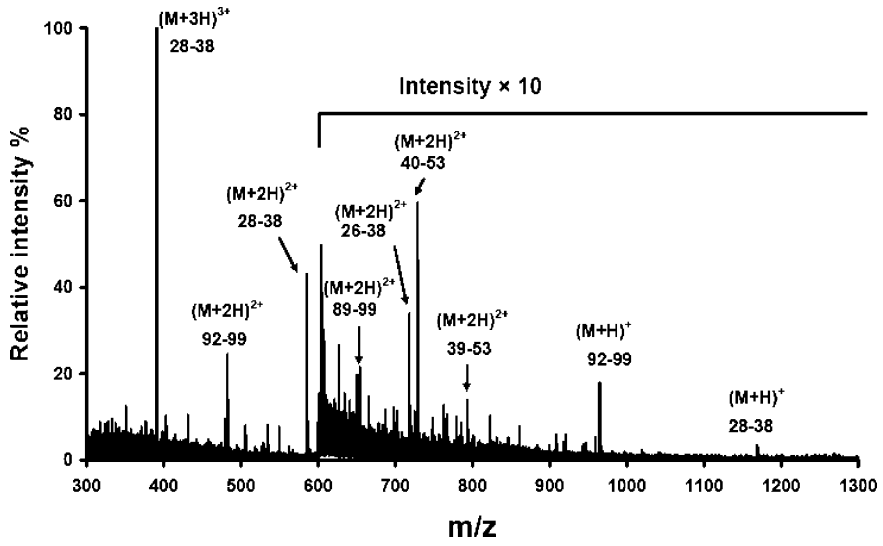

Fig. 12. Mass spectrum corresponding to the injection peak on the MS trace obtained for separation test carried out using the on-microsystem monolithic column. Arrows indicate the identified peptides from the Cyt C digest. The intensity is multiplied by 10 above *m/z* 600.

a Cytochrome *C* digest sample at 800–0.08 fmol/μl, 1 μl being injected into the column. A poorer separation of the Cyt C fragments was achieved on the monolithic column prepared in the microchannel in spite of the relative high pressure drop that was measured during the separation tests. Fig. 12 represents the mass spectrum averaged over the elution peak. It is noteworthy that the peptides were efficiently desalted on the monolithic column but that most of the peptides were eluted in the injection peak. However, there were major changes here compared to the capillary format that could account for these results. Not only the total porosity of the monolithic phase was higher in the microchannel as in the capillary format, 70% against 60% volume in the capillary format, but the inner wall preliminary treatment was suppressed here and the column dimensions were dramatically changed. Hence, the observed low performances of the monolithic column could be accounted for by the following points. Firstly, as the porogenic content was increased, the resulting monolithic phase was more porous and consequently, its separation ability was lower. Secondly, the microchannel inner walls were not treated so as to secure the covalent anchoring of the monolith in its support; thus, there may be some fissuring at the inner wall proximity through which samples could flow without interacting with the monolithic stationary phase and its hydrophobic groups. Lastly, and surely, mainly, the column dimensions were dramatically changed compared to the case in the capillary format; in the microsystem, the column dimensions were a section area of $A_{\text{channel}} = l \times d$ with l and d being respectively of 100 and 200 μm (2×10^4 μm^2) and a length of 2.2 cm against a circular section area of $A_{\text{capillary}} = \pi r^2$ with an inner diameter being of 75 μm (0.44×10^4 μm^2) and a column length of 17 cm in the capillary format. As well known, the chromatographic separation techniques are sensitive to the A_{section}/L ratio for the column; the lower this ratio, the better the separation. The 35-fold increase of this ratio from the capillary to the microchannel format was apparently the main reason why a poor separation was achieved on the monolithic phase. A microsystem with optimized dimensions is currently under development and fabrication so as to improve these results.

4. Conclusion

In this paper we described the successful preparation of a monolithic phase, which was based on LMA as functional monomer and a cyclohexanol/ethylene glycol mixture as porogen in a capillary format for chromatographic purposes. This monolithic column was first tested in nanoLC/MS for the separation of a Cytochrome *C* digest sample at 800 and 80 fmol in a capillary format. The column was seen to exhibit separation capabilities and quality close to these obtained with a commercial column using the 800 fmol sample. However, using 80 fmol of Cyt C digest, the separation was outstanding, as the column was not saturated anymore as demonstrated by the higher efficiency values *N*. Nonetheless, the low-level peptides were more difficult to be detected and identified in MS. Lastly a polymer monolithic column was successfully prepared in a SU-8-based microfabricated channel and also tested for the separation of the Cyt C digest sample. The column dimensions afford a poor separation of the Cyt C fragments, but the system including the monolithic column was robust and was able to withstand high pressure values for 24 h at a time.

Acknowledgements

The authors would like to thank the French network for micro- and nanotechnologies for their financial support for this work (*Integrated Proteomics* project) as well as the

GenHomme network (*BioChipLab* consortium). The Mass Spectrometry facilities used for this study is funded by the European community (FEDER), the Région Nord-Pas de Calais (France), the CNRS and the Université des Sciences et Technologies de Lille. We also would like to thank Christophe Boyaval from the IEMN for the SEM images and Dr Steve Arscott from the IEMN for his kind help to design and fabricate the SU-8-based microsystem.

References

[1] D.R. Reyes, D. Iossifidis, P.A. Auroux, A. Manz, Anal. Chem. 74 (2002) 2623.
[2] P.A. Auroux, D. Iossifidis, D.R. Reyes, A. Manz, Anal. Chem. 74 (2002) 2637.
[3] G. Marko-Varga, J. Nilsson, T. Laurell, Electrophoresis 24 (2003) 3521.
[4] N. Lion, T.C. Rohner, L. Dayon, I.L. Arnaud, E. Damoc, N. Youhnovski, Z.-y. Wu, C. Roussel, J. Josserand, H. Jensen, J.S. Rossier, M. Przybylski, H.H. Girault, Electrophoresis 24 (2003) 3533.
[5] S. Le Gac, S. Arscott, C. Rolando, Electrophoresis 24 (2003) 3640.
[6] J.P. Kutter, TrAC, Trends Anal. Chem. 19 (2000) 352.
[7] M. Wilm, M. Mann, Anal. Chem. 68 (1996) 1.
[8] E.X. Vrouwe, J. Gysler, U.R. Tjaden, J. Van der Greef, Rapid Commun. Mass Spectrom. 14 (2000) 1682.
[9] E. Varesio, S. Rudaz, K.-H. Krause, J.-L. Veuthey, J. Chromatogr. A 974 (2002) 135.
[10] A.R. Ivanov, C. Horvath, B.L. Karger, Electrophoresis 24 (2003) 3663.
[11] G. Ocvirk, E. Verpoorte, A. Manz, M. Grasserbauer, H.M. Widmer, Anal. Methods Instrum. 2 (1995) 74.
[12] H. Andersson, C. Jonsson, C. Moberg, G. Stemme, Electrophoresis 22 (2001) 3876.
[13] B. He, L. Tan, F. Regnier, Anal. Chem. 71 (1999) 1464.
[14] J.-L. Liao, N. Chen, C. Ericson, S. Hjerten, Anal. Chem. 68 (1996) 3468.
[15] H. Andersson, W. Van der Wijngaart, G. Stemme, Electrophoresis 22 (2001) 249.
[16] L. Ceriotti, N.F. de Rooij, E. Verpoorte, Anal. Chem. 74 (2002) 639.
[17] B. He, F. Regnier, J. Pharm. Biomed. Anal. 17 (1998) 925.
[18] B. He, N. Tait, F. Regnier, Anal. Chem. 70 (1998) 3790.
[19] E.C. Peters, F. Svec, J.M.J. Frechet, Adv. Mater. 11 (1999) 1169.
[20] F. Svec, J.M.J. Frechet, Chem. Mater. 7 (1995) 707.
[21] J.J. van Deemter, F.J. Zuiderweg, A. Klinkenberg, Chem. Eng. Sci. 5 (1956) 271.
[22] C. Viklund, F. Svec, J.M.J. Frechet, K. Irgum, Chem. Mater. 8 (1996) 744.
[23] F. Svec, J.M.J. Frechet, Ind. Eng. Chem. Res. 38 (1999) 34.
[24] F. Svec, J.M.J. Frechet, Macromolecules 28 (1995) 7580.
[25] S. Xie, F. Svec, J.M.J. Frechet, J. Chromatogr. A 775 (1997) 65.
[26] A. Premstaller, H. Oberacher, W. Walcher, A.M. Timperio, L. Zolla, J.-P. Chervet, N. Cavusoglu, A. van Dorsselaer, C.G. Huber, Anal. Chem. 73 (2001) 2390.
[27] M. Xu, D.S. Peterson, T. Rohr, F. Svec, J.M.J. Frechet, Anal. Chem. 75 (2003) 1011.
[28] A.R. Ivanov, L. Zang, B.L. Karger, Anal. Chem. 75 (2003) 5306.
[29] F. Svec, J.M.J. Frechet, J. Chromatogr. A 702 (1995) 89.
[30] Z. Pan, H. Zou, W. Mo, X. Huang, R. Wu, Anal. Chim. Acta 466 (2002) 141.
[31] M. Zhang, Z. El Rassi, Electrophoresis 22 (2001) 2593.
[32] D. Josic, A. Buchacher, J. Biochem. Biophys. Methods 49 (2001) 153.
[33] B. Barroso, D. Lubda, R. Bischoff, J. Proteome Res. 2 (2003) 633.
[34] T.J. Shepodd, US Patent 6 472 443 (2002);
T.J. Shepodd, Chem. Abstr. 137 (2002) 326337.
[35] C. Yu, F. Svec, J.M.J. Frechet, Electrophoresis 21 (2000) 120.
[36] C. Yu, M.H. Davey, F. Svec, J.M.J. Frechet, Anal. Chem. 73 (2001) 5088.
[37] T. Rohr, C. Yu, M.H. Davey, F. Svec, J.M.J. Frechet, Electrophoresis 22 (2001) 3959.
[38] G. Jas, A. Kirschning, Chem. Eur. J. 9 (2003) 5708.
[39] D.J. Throckmorton, T.J. Shepodd, A.K. Singh, Anal. Chem. 74 (2002) 784.
[40] J. Carlier, S. Arscott, V. Thomy, J.-C. Fourrier, F. Caron, J.-C. Camart, C. Druon, P. Tabourier, J. Micromech. Microeng. 14 (2004) 619.
[41] A.E. Rodrigues, V.G. Mata, M. Zabka, L. Pais, J. Chromatogr. Lib. 67 (2003) 325.
[42] I. Gusev, X. Huang, C. Horvath, J. Chromatogr. A 855 (1999) 273.
[43] N. Vervoort, P. Gzil, G.V. Baron, G. Desmet, Anal. Chem. 75 (2003) 843.
[44] A. Wang, W. Carr, J. Chromatogr. A 965 (2002) 3.